RSC Advances

PAPER

View Article Online
View Journal | View Issue

Cite this: *RSC Adv.*, 2024, **14**, 37131

Antileishmanial potential of thiourea-based derivatives: design, synthesis and biological activity†

Abdul Hadi,[abc] Muhammad Yaqoob,[d] Fahad Hussain,[d] Yasser M.S.A Al-Kahraman,*[a] Muhammad Saeed Jan,[e] Abid Mahmood,[f] Thomas Shier[c] and Umer Rashid *[d]

Received 9th July 2024
Accepted 4th November 2024

DOI: 10.1039/d4ra04965a

rsc.li/rsc-advances

Leishmaniasis is a neglected tropical disease caused by protozoan parasites and transmitted to humans by the sandfly vector. Currently, the disease has limited therapeutic alternatives. Thiourea derivatives were designed, synthesized, and screened for antileishmanial activity. The synthesized compounds **4g**, **20a**, and **20b** demonstrated significant *in vitro* potency against *L. major*, *L. tropica*, and *L. donovani* promastigotes with IC_{50} values at low submicromolar concentrations. Compound **4g** showed the highest activity against the amastigotes of *L. major*. In enzyme inhibition assays, compounds **4g**, **20a**, and **20b** demonstrated good inhibitory potential against *L. major* dihydrofolate reductase (DHFR) and pteridine reductase 1 (PTR1). Reversal of the antileishmanial effect by adding folic acid revealed that the compounds **4g**, **20a**, and **20b** act through an antifolate mechanism. Cytotoxicity data on normal human embryonic kidney cells (HEK-293) showed that the synthesized compounds displayed better safety profiles. Docking experiments on the enzymes *L. major* DHFR and PTR1 demonstrated the significant interactions with the active pocket residues of the target enzymes.

Introduction

The parasitic disease leishmaniasis is a neglected tropical disease (NTD) mainly caused by twenty species of *Leishmania*. All *Leishmania* infections commence with the sandfly bite, which introduces the protozoan parasite into the host's blood through the skin during its blood feeding. Every year about one million people get affected by leishmaniasis, which is becoming a social, health, and economic burden on many countries in subtropical regions. In the Middle East, Northwestern China, and Northern Africa, the main cause of cutaneous leishmaniasis is *Leishmania major*.[1–5]

The symptoms of leishmaniasis depend upon the clinical form, *i.e.*, cutaneous and visceral, and the type of the species.[6] The three well-known clinical forms are cutaneous leishmaniasis abbreviated as CL, mucocutaneous leishmaniasis abbreviated as MCL and visceral leishmaniasis, also called kala-azar, abbreviated as VL.[7] Post-kala-azar dermal leishmaniasis abbreviated as PKDL is the least common clinical form of the disease.[8] The general symptoms are skin rashes, erythema, and papules that later become scars as seen in CL and fever, black spots on the skin, and enlargement of the spleen as seen in visceral leishmaniasis.[8,9] Besides the skin, other parts of the body, such as the ears, lips, mucosa of the nose, and mouth, are also affected by leishmaniasis.[10] The disease is widely distributed in the tropics as well as subtropics.[11] In the US, leishmania cases are diagnosed among travellers to endemic regions, armed forces from the military, and immigrants.[12] In the life cycle of *Leishmania*, the parasite protozoan experiences a digenetic style, *i.e.*, promastigotes and amastigotes.[13] The promastigote forms of the parasite multiply extracellularly in the vector's digestive tract or gut and are transmitted to the mammalian cells during the vector's blood-feeding meal, where they convert into amastigote forms, which are responsible for the clinical manifestation of leishmaniasis.[14]

The proliferation and growth of the *Leishmania* parasite are affected by different metabolic pathways. The metabolic pathway related to folate plays a crucial role in the biochemical processes; it depends on reduced pterin and tetrahydrofolate as essential cofactors. Hence, the most suitable targets associated with the folate metabolic pathway include pteridine reductase-1 and dihydrofolate reductase. An NADPH-dependent key enzyme called DHFR in the folate metabolism is responsible for the formation of deoxythymidine monophosphate (dTMP) from

[a]*Department of Pharmacy, COMSATS University Islamabad, Abbottabad Campus, 22060 KPK, Pakistan. E-mail: yasser@cuiatd.edu.pk*
[b]*Faculty of Pharmacy and Health Sciences, University of Balochistan, Quetta 08770, Pakistan*
[c]*Department of Medicinal Chemistry, University of Minnesota, Minneapolis, USA*
[d]*Department of Chemistry, COMSATS University Islamabad, Abbottabad Campus, 22060 KPK, Pakistan. E-mail: umerrashid@cuiatd.edu.pk*
[e]*Department of Pharmacy, Bacha Khan University, 24420, Charsadda, KPK, Pakistan*
[f]*Department of Pharmaceutical Chemistry, Government College University Faisalabad, Pakistan*

† Electronic supplementary information (ESI) available. See DOI: https://doi.org/10.1039/d4ra04965a

deoxy-uridine monophosphate (dUMP) and the conversion of dihydrofolate/folate to tetrahydrofolate. Thus, biosynthesis of thymidine and subsequent DNA biosynthesis can be prevented by the inhibition of DHFR, and as a result, this will disturb the parasite's folate metabolic pathway in *Leishmania*, which leads to the death of the parasite.[5,15–18]

Currently, the basis of antileishmanial treatment is chemotherapy. Different drug options are available and the choice of medication differs according to the disease state, parasite form, and geographic location.[19] Drugs already available for treatment purposes are pentavalent antimonials (I.V), miltefosine (oral), pentamidine (intramuscular), liposomal amphotericin B (I.M and I.V), and paromomycin (topical). These drug candidates are in general associated with undesirable complications such as organ toxicity, teratogenicity, prolonged hospital stay, and reaction at the injection site. In addition, high costs and resistance remain the most important issues.[10] Therefore, there is a need to seek alternative drug candidates and explore new therapeutic interventions to improve the existing therapy.

Several heterocyclic scaffolds such as triazole, imidazole, pyrazole, quinoline, pyrimidine, quinazoline, benzimidazole, pyrrole, and indole are being evaluated for the treatment of leishmaniasis.[20,21] Moreover, *N*-acyl/dimeric *N*-arylpiperazine and halogen-rich salicylanilides have also been reported as potential antileishmanial agents.[22,23] Thiourea, an organosulfur compound, is known for its therapeutic uses, including treating co-infections, acting as an antioxidant, exhibiting antibacterial activity, and showing anti-cancer properties.[24] Thiourea derivatives were screened against parasitic protozoa for exploring their anti-amoebic and anti-leishmanial properties.[25] Thiourea derivatives have been shown to inhibit both the wild-type and the resistant mutant forms of Plasmodium falciparum PfDHFR.[26] Moreover, compounds belonging to the thiourea group (**I–IV**) have also been reported in the literature as antileishmanial therapeutics (Fig. 1). The cyclic propane derivatives of thiourea were screened against the promastigote form of *L. major* and showed significant antileishmanial potential.[27] Other compounds of the thiourea class include **II** and **III**, which have also demonstrated antileishmanial potential against *L. major*.[28] Compound **IV**, which is the basis of the rationale for the current study, was screened against both promastigote and amastigote forms of *L. major* and demonstrated efficient EC_{50} values with a good safety profile on mammalian cell lines.[29] The compound (**IV**) possesses the thiourea functional group as its important constituent where only one hydrogen atom of the NH_2 group of the thiourea moiety is substituted by an aromatic system.

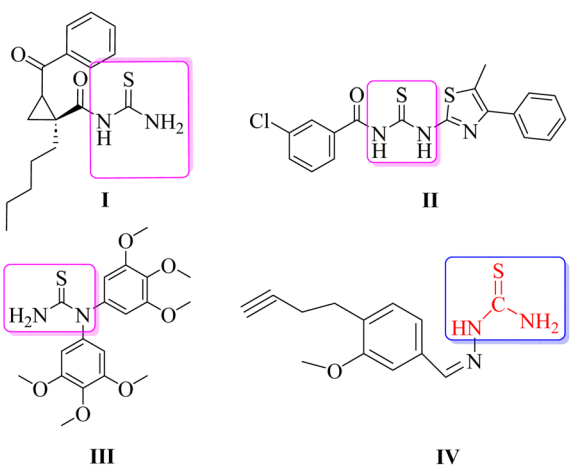

Fig. 1 Thiourea derivatives reported against leishmaniasis. Structure IV is chosen for the rationale of the current study.

Materials and methods

General information

All the chemicals and reagents were obtained from commercial sources (Sigma-Aldrich and Merck) and used without any further purification. Melting points of the compounds were determined on the Stuart SMP10 apparatus. Reactions were monitored by thin-layer chromatography (TLC) using silica gel aluminium sheets. To determine the molecular mass, high-resolution mass spectrometry was carried out using Bruker Daltonics TSQ Quantum Classic LC-MS equipment at the Chemistry Department, University of Minnesota, USA. Only a positive method was used for ionization with the polymer PEG 300 or PPG 420. Proton (^{1}H) and carbon (^{13}C) NMR were taken using 400 MHz and 100 MHz, spectrometer, respectively. The chemical shift values and coupling constants were presented as delta (δ) in ppm and J in Hz, respectively. The multiplicities were represented by 's' for singlet, 'd' for doublet, 't' for triplet, and 'q' for quintet. Analytical grade acetone, methanol, ethanol, chloroform, dimethyl sulfoxide (DMSO), and *n*-hexane were used to synthesize the designed thiourea derivatives. Molecular sieves of 3 Å size were heat-activated and used for the drying of acetone.

Reaction procedure for the synthesis of thiourea derivatives (4a–4h and 5a–5d)

The thiourea derivatives were synthesized according to the previous method with slight modification.[30] To the aromatic carboxylic acid (3 mmol) was added thionyl chloride (324 μL, 4.5 mmol). The mixture was heated to reflux along with stirring for 1 to 2 h. The resulting acid chloride was cooled to room temperature and dissolved in dry acetone. Then 3 mmol (292 mg) potassium thiocyanate was added to the solution and stirred for 2 h. Equimolar aromatic secondary amines and substituted anilines were added to the organic isothiocyanate mixture and refluxed for 3 to 4 hours to get the final product thiourea. The mixture was cooled, filtered, and washed with cold water. Finally, the product was dried and recrystallized with ethanol or methanol.

(*N*-((4-Methoxyphenyl)carbamothioyl)furan-2-carboxamide) (4a). Off-white solid, yield: 73%, molecular weight 276.31, m.p. 99–101 °C, ^{1}H NMR (400 MHz, $CDCl_3$): δ 3.79 (s, 3H, methoxy-H), 6.53 (d, J = 2.8 Hz, 1H, furan-C_2–H), 6.88 (d, J = 8.5 Hz, 2H, benzene-$C_{9,11}$–H), 7.20 (d, J = 3.5 Hz, 1H, furan-C_3–H), 7.48 (s, 1H, furan-C_1–H), 7.54 (d, J = 8.5 Hz, 2H, benzene-$C_{8,12}$–H), 7.98 (s, 1H, thiourea-NH–H), ^{13}C NMR (100 MHz, DMSO-d_6) δ ppm: 55.4 (methoxy-C), 77.2, 112.5, 114.2, 114.9, 121.6, 130.3,

144.0, 147.9 (Ar–C), 155.9 (C=O), 176.5 (thiourea C=S), anal. calcd for $C_{13}H_{12}N_2O_3S$, C, 56.51; H, 4.38; N, 10.14; O, 17.37; S, 11.60, found C, 56.49; H, 4.37; N, 10.11; O, 17.31; S, 11.57, HRMS: *m*/*z*: 299.0178 $[M + Na]^+$.

(*N*-((2-Hydroxyphenyl)carbamothioyl)furan-2-carboxamide) (4b). Light brown solid, yield 72%, molecular weight 262.28, m.p. 191–193 °C, ^{1}H NMR (400 MHz, DMSO-d_6) δ 6.58 (dd, J = 5.1, 1.5 Hz, 1H, furan-C_2–H), 6.88 (dd, J = 8.4, 1.6 Hz, 1H, benzene-C_{11}–H), 7.12–6.97 (m, 2H, benzene-$C_{9,8}$–H), 7.38 (dd, J = 5.2, 1.6 Hz, 1H, furan-C_3–H), 7.67 (dd, J = 8.0, 1.6 Hz, 1H, benzene-C_8–H), 7.71 (t, J = 1.7 Hz, 1H, furan-C_1–H), 8.35 (s, 1H, C_{12}-hydroxyl-H), 10.55 (s, 1H, thiourea-NH–H), 11.26 (s, 1H, thiourea-NH–H), ^{13}C NMR (100 MHz, DMSO-d_6) δ ppm: 112.7, 115.4, 116.6, 121.6, 123.8, 125.5, 128.3, 145.6, 150.3, 150.8 (Ar–C), 160.3 (C=O), 179.2 (C=S), anal. calcd for $C_{12}H_{10}N_2O_3S$; C, 54.95; H, 3.84; N, 10.68; O, 18.30; S, 12.22, found C, 54.90; H, 3.80; N, 10.67; O, 18.27; S, 12.19, HRMS: *m*/*z*: 285.1198 $[M + Na]^+$.

(*N*-((3-Hydroxyphenyl)carbamothioyl)furan-2-carboxamide) (4c). Dark yellow solid, yield 87%, molecular weight 262.28, m.p. 175–176 °C, NMR (400 MHz, $CDCl_3$) δ 5.19 (s, 1H, C_{11} phenyl hydroxy-H), 6.63 (dd, J = 3.7, 1.7 Hz, 1H, furan-C_2–H), 6.75 (dd, J = 8.0, 2.4 Hz, 1H, phenol-C_8–H), 7.12 (dd, J = 8.4, 1.7 Hz, 1H, phenol-C_{12}-H), 7.24 (d, J = 16.1 Hz, 1H, phenol-C_9–H), 7.38 (d, J = 3.7 Hz, 1H, furan-C_3–H), 7.45 (t, J = 2.2 Hz, 1H, furan-C_1–H), 7.64–7.59 (m, 1H, phenol-C_{10}–H), 9.17 (s, 1H, thiourea-NH–H), 12.30 (s, 1H, thiourea-NH–H); ^{13}C NMR (100 MHz, $CDCl_3$) δ ppm, 108.5, 110.2, 112.7, 115.7, 116.6, 130.3, 140.0, 145.6, 150.8 (Ar–C), 157.9 (C–OH), 160.3 (C=O), 178.4 (thiourea C=S); anal. calcd for $C_{12}H_{10}N_2O_3S$; C, 54.95; H, 3.84; N, 10.68; O, 18.30; S, 12.22, found, C, 54.90; H, 3.80, N, 10.67; O, 18.27; S, 12.20, HRMS: *m*/*z*: 285.0317 $[M + Na]^+$.

4-(3-(Furan-2-carbonyl)thioureido)benzoic acid (4d). Yellow color solid, yield 77%, molecular weight 290.29, m.p. 275–277 °C, ^{1}H NMR (400 MHz, DMSO-d_6); δ 6.73 (dd, J = 3.7, 1.7 Hz, 1H, furan-C_2–H), 7.86–7.79 (m, 3H, $C_{8,12,3}$–H), 7.97–7.90 (m, 2H, benzene-$C_{9,11}$–H), 8.04 (dd, J = 1.7, 0.8 Hz, 1H, furan-C_1–H), 11.35 (s, 1H, thiourea-NH–H), 12.49 (s, 1H, thiourea-NH–H), ^{13}C NMR (100 MHz, DMSO-d_6) δ ppm, 112.6, 116.6, 121.1 (Ar–C), 126.7 (C–COOH), 130.5, 141.4, 145.5, 150.7(Ar–C), 160.2 (C=O), 168.4 (C=O–OH), 178.5 (thiourea C=S), anal. calcd for, $C_{13}H_{10}N_2O_4S$; C, 53.79; H, 3.47; N, 9.65; O, 22.05; S, 11.04, found C, 53.69; H, 3.41; N, 9.59; O, 22.09; S, 11.09. HRMS: *m*/*z*: 313.0252 $[M + Na]^+$.

(*N*-((4-Methoxyphenyl)carbamothioyl)thiophene-2-carboxamide) (4e). Light yellow solid, yield 71%, molecular weight 292.37, m.p. 175–176 °C, ^{1}H NMR (400 MHz, DMSO-d_6) δ 3.78 (s, 3H, methoxy-H), 6.96–6.88 (m, 2H, phenol-C_{8-12}–H), 7.21 (dd, J = 6.5, 5.4 Hz, 1H, thiophene-C_2–H), 7.62–7.54 (m, 2H, benzene-$C_{9,11}$–H), 7.97 (dd, J = 5.4, 1.7 Hz, 1H, thiophene-C_1–H), 8.21 (dd, J = 6.5, 1.6 Hz, 1H, thiophene-C_3–H), 11.40 (s, 1H, thiourea-NH–H), 11.48 (s, 1H, thiourea-NH–H), ^{13}C NMR (100 MHz, DMSO-d_6) δ ppm; 55.33 (methoxy-C), 114.4, 126.5, 128.0, 129.6, 130.9, 132.2, 138.5 (Ar–C), 156.3 (C–O), 162.5(C=O), 178.3 (thiourea C=S); anal. calcd for $C_{13}H_{12}N_2O_2S_2$, C, 53.41; H, 4.14; N, 9.58; O, 10.94; S, 21.93, found, C, 53.39; H, 4.11; N, 9.54; O, 10.92; S, 21.90, HRMS: *m*/*z*: 315.0300 $[M + Na]^+$.

(*N*-((2-Hydroxyphenyl)carbamothioyl)thiophene-2-carboxamide) (4f). Dark yellow solid, yield 70%, molecular weight 278.34, m.p. 228–229 °C, ^{1}H NMR (400 MHz, DMSO-d_6) δ ppm; 6.79 (td, J = 7.8, 1.4 Hz, 1H, phenol-C_{11}–H), 6.89 (dd, J = 8.1, 1.4 Hz, 1H, thiophene-C_2–H), 7.03 (td, J = 7.7, 1.6 Hz, 1H, phenol-C_{10}–H), 7.22–7.16 (m, 1H, phenol-C_8–H), 7.94 (d, J = 4.9 Hz, 1H, phenol-C_9–H), 8.23 (d, J = 3.9 Hz, 1H, thiophene-C_1–H), 8.40 (dd, J = 8.1, 1.6 Hz, 1H, thiophene-C_3–H), 10.44 (s, 1H, C_{12}–hydroxyl group–H), 11.36 (s, 1H, thiourea-NH–H), 12.70 (s, 1H, thiourea-NH–H), ^{13}C NMR (100 MHz, DMSO-d_6) δ ppm; 115.5, 118.8, 123.7, 126.1, 127.1, 129.2, 133.0, 135.7, 136.7 (Ar–C), 149.3 (C–OH), 162.5 (C=O), 177.6 (thiourea C=S), analysis calcd for $C_{12}H_{10}N_2O_2S_2$; C, 51.78; H, 3.62; N, 10.06; O, 11.50; S, 23.04, found, C, 51.71; H, 3.58; N, 10.09; O, 11.48; S, 23.09, HRMS: *m*/*z*: 301.1078 $[M + Na]^+$.

(*N*-((3-Hydroxyphenyl)carbamothioyl)thiophene-2-carboxamide) (4g). Light yellow solid, yield 77%, molecular weight 278.34, m.p. 190–191 °C, ^{1}H NMR (400 MHz, DMSO-d_6) δ 6.63 (dd, J = 8.1, 2.4 Hz, 1H, phenol-C_{10}-H), 6.98 (dd, J = 7.9, 2.0 Hz, 1H, phenol-C_8–H), 7.16 (t, J = 8.0 Hz, 1H, thiophene-C_2–H), 7.24–7.16 (m, 2H, phenol-$C_{9,12}$–H), 7.99 (dd, J = 4.9 Hz, 1H, thiophene-C_1–H), 8.31 (d, J = 3.9 Hz, 1H, thiophene-C_3–H), 9.68 (s, 1H, C_{11}–hydroxyl-OH–H), 11.48 (s, 1H, thiourea-NH–H), 12.36 (s, 1H, thiourea-NH–H), ^{13}C NMR (100 MHz, DMSO-d_6) δ ppm; 115.5, 118.8, 123.7, 126.1, 127.1, 129.2, 133.0, 135.7, 136.7 (Ar–C), 149.3 (C–OH), 162.5 (C=O), 177.6 (thiourea C=S), anal. calcd for $C_{12}H_{10}N_2O_2S_2$, C, 51.78; H, 3.62; N, 10.06; O, 11.50; S, 23.04, found, C, 51.73; H, 3.59; N, 10.01; O, 11.45; S, 23.07, HRMS: *m*/*z*: 301.1078 $[M + Na]^+$.

4-(3-(Thiophene-2-carbonyl)thioureido)benzoic acid (4h). White solid, yield 78%, molecular weight 306.35, m.p. 268–269 °C, ^{1}H NMR (400 MHz, DMSO-d_6) δ 7.21 (dd, J = 5.0, 3.7 Hz, 1H, thiophene-C_2–H), 7.91–7.80 (m, 3H, thiophene-C_1, benzoic acid –$C_{9,11}$-H), 7.98–7.87 (m, 2H, benzoic acid-$C_{8,12}$-H), 8.03 (dd, J = 3.8, 1.2 Hz, 1H, thiophene-C_3–H), 10.44 (s, 1H, thiourea-NH–H), 12.73 (s, 1H, thiourea-NH–H), ^{13}C NMR (100 MHz, DMSO-d_6) δ 180.3 (thiourea C=S), (160.6 carbonyl–C=O), 143.3, 140.0, 135.9, 133.2, 132.8, 130.7, 130.3, 130.1, 128.5, 123.9, 119.8 (Ar–C) anal. calcd for $C_{13}H_{10}N_2O_3S_2$, C, 50.97; H, 3.29; N, 9.14; O, 15.67; S, 20.93, found, C, 50.94; H, 3.26; N, 9.10; O, 15.64; S, 20.91, HRMS: *m*/*z*: 329.0124 $[M + Na]^+$.

***N*-(Pyridin-2-ylcarbamothioyl)furan-2-carboxamide (5a).** Light orange solid, yield 75%, molecular weight 247.27, m.p. 225–226 °C; ^{1}H NMR (400 MHz, DMSO-d_6) δ 6.74 (dd, J = 3.6, 1.7 Hz, 1H, furan-C_2–H), 7.23 (t, J = 6.3 Hz, 1H, pyridine-C_{10}-H), 7.56 (t, 1H, pyridine-C_9–H), 7.87 (td, J = 7.8, 1.9 Hz, 1H, furan-C_3–H), 8.05 (d, J = 1.7 Hz, 1H, furan-C_1–H), 8.42 (dd, J = 5.0, 1.8 Hz, 1H, pyridine-C_{11}-H), 8.68 (t, 1H, pyridine-C_8–H), 11.40 (s, 1H, thiourea-NH–H), 12.97 (s, 1H, thiourea-NH–H). ^{13}C NMR (100 MHz, DMSO-d_6) δ, 177.85 (thiourea-C=S), (156.01, carbonyl C=O), 147.6, 139.9, 135.0, 119.0, 117.5, 117.4, 113.2, 112.9, 31.1, Ar–C), anal. calcd for $C_{11}H_9N_3O_2S$ C, 53.43; H, 3.67; N, 16.99; O, 12.94; S, 12.97, found, C, 53.39; H, 3.63; N, 16.96; O, 12.90; S, 12.94, HRMS: *m*/*z*: 270.0301 $[M + Na]^+$.

(*N*-(Thiazol-2-ylcarbamothioyl)furan-2-carboxamide) (5b). Light yellow solid, yield 79%, molecular weight 253.29, m.p.

196–197 °C, ^{1}H NMR (400 MHz, DMSO-d_6): δ 6.58 (dd, J = 5.1, 1.5 Hz, 1H, furan-C_2–H), 6.78 (d, J = 4.4 Hz, 1H, thiazole-C_9–H), 7.12 (d, J = 4.6 Hz, 1H, thiazole-C_8–H), 7.32 (dd, J = 5.2, 1.6 Hz, 1H, furan-C_3–H), 7.81 (t, J = 1.7 Hz, 1H, furan-C_1–H), 11.44 (s, 1H, thiourea-NH–H), 11.82 (s, 1H, thiourea-NH–H), ^{13}C NMR (100 MHz, DMSO-d_6) δ ppm: 111.6, 112.7, 116.6, 135.3, 145.6, 150.8, 160.4 (Ar–C), 161.6 (C=O), 176.4 (thiourea C=S), anal. calcd for $C_9H_7N_3O_2S_2$; C, 42.68; H, 2.79; N, 16.59; O, 12.63; S, 25.31, found, C, 42.63; H, 2.75; N, 16.57; O, 12.60; S, 25.29, HRMS: m/z: 276.0191 $[M + Na]^+$.

***N*-(Pyridin-2-ylcarbamothioyl)thiophene-2-carboxamide (5c).** Orange solid, yield 73%, molecular weight 297.78, m.p. 195–196 °C, ^{1}H NMR (400 MHz, DMSO-d_6) δ 7.24 (ddt, J = 5.0, 3.7, 2.3 Hz, 1H, thiophene-C_2–H), 7.48 (ddd, J = 8.0, 4.7, 1.1 Hz, 1H, benzene-C_8–H), 8.05 (dd, J = 5.0, 1.2 Hz, 1H, thiophene-C_3–H), 8.31 (dt, J = 4.8, 1.5 Hz, 1H, benzene-C_9–H), 8.42–8.34 (m, 2H, benzene-C_{10}, thiophene-C_1–H (m), 11.94 (s, 1H, thiourea-NH–H), 12.51 (s, 1H, thiourea-NH–H), ^{13}C NMR (100 MHz, DMSO-d_6) δ 180.7, thiourea C=S), 162.7 (carbonyl C=O), 147.8, 146.2, 137.4, 136.7, 136.2, 133.6, 133.2, 129.2, 123.6 (Ar–C), anal. calcd for, $C_{11}H_9N_3OS_2$, C, 44.37; H, 2.71; Cl, 11.90; N, 14.11; O, 5.37; S, 21.53, found, C, 44.31; H, 2.66; Cl, 11.88; N, 14.08; O, 5.35; S, 21.49, HRMS: m/z: 285.9771 $[M + Na]^+$.

(*N*-(Thiazol-2-ylcarbamothioyl)thiophene-2-carboxamide) (5d). Light yellow color solid, yield 75%, molecular weight 269.36, m.p. 188–189, ^{1}H NMR (400 MHz, DMSO-d_6) δ 7.24 (dd, J = 5.0, 3.9 Hz, 1H, thiophene-C_2–H), 7.31 (d, J = 3.5 Hz, 1H, thiazol-C_{10}–H), 7.62 (dd, J = 3.6 Hz, 1H, thiophene-C1–H), 8.09–8.02 (m, 1H, thiazol-C_9–H), 8.37 (dd, J = 3.9 Hz, 1H, thiophene-C_3–H), 12.09 (s, 1H, thiourea-NH–H), 13.99 (s, 1H, thiourea-NH–H), ^{13}C NMR (100 MHz, DMSO-d_6) δ ppm 111.9, 128.0, 129.6, 132.2, 135.5, 138.7, 161.6 (Ar–C), 162.6 (C=O), 176.6 (thiourea C=S), anal. calcd for $C_9H_7N_3OS_3$, C, 40.13; H, 2.62; N, 15.60; O, 5.94; S, 35.71, found, C, 40.11; H, 2.59; N, 15.57; O, 5.89; S, 35.73, HRMS: m/z: 292.0660 $[M + Na]^+$.

General procedure for the synthesis of 1-(3-oxo-butanoyl) piperidine-4-carboxylic acid (8)

Synthesis of compound **8** was carried out by using our previously reported procedure.[4] A mixture of piperidine-4-carboxylic acid (7) and ethyl acetoacetate was heated under reflux in absolute ethanol as the solvent. After completion of the reaction, the reaction mixture was cooled. Ethanol was evaporated and the crude material was purified by using silica gel chromatography (*n*-hexane/ethyl acetate, 20 : 1).

Transparent liquid, yield 80%, ^{1}H NMR (400 MHz, $CDCl_3$) δ 12.07 (s, 1H, –OH), 3.89 (s, 2H, –CH_2), 3.27–3.19 (m, 4H, 2× pip-CH_2), 3.09–3.04 (m, 1H, pip-CH), 2.69 (s, 3H, CH_3), 2.24–2.17 (m, 2H, pip-CH_2), 1.76–1.62 (m, 2H, pip-CH_2).

General procedure for the synthesis of 1-(2-amino-4-methyl-6-phenylpyrimidine-5-carbonyl)piperidine-4-carboxylic acid (15)

Our previously reported multistep protocol was followed for the synthesis of 2-aminopyrimidine **15**.[31,32] The traditional Biginelli reaction was used to synthesize compound **12**. Pyridinium chlorochromate (PCC) oxidised compound **12** into compound **13**. Dihydropyrimidine (**12**, 5 mmol) was stirred with 30 mmol of PCC in DCM. Following the completion of the reaction (TLC, 15 hours), the solvent was removed, and silica gel chromatography (CH_2Cl_2/CH_3OH, 9 : 1) was used to purify the crude product. Compound **13** (10 mmol) was then refluxed for 30 to 45 minutes in $POCl_3$. After that, the reaction mixture was distilled to get rid of $POCl_3$. The obtained crude product was purified using silica gel chromatography (DCM/CH_3OH, 10 : 1). Compound **14** (10 mmol) was suspended in acetone. After adding 20 mmol of ammonium acetate, the mixture was stirred for three to four hours at RT. Compound **15** was obtained by filtering out the resultant precipitates and washing and drying them with diethyl ether.

White solid, yield 63%, m.p. 145–147 °C, ^{1}H NMR (400 MHz, $CDCl_3$) δ 12.07 (s, 1H, –OH), 7.37–7.28 (m, 5H, ArH), 6.69 (s, 2H, NH_2), 3.78–3.70 (m, 2H, pip-CH_2), 3.64–3.57 (m, 2H, pip-CH_2), 3.06–3.03 (m, 1H, pip-CH), 2.56 (s, 3H, CH_3), 2.39–2.30 (m, 2H, pip-CH_2), 1.92–1.84 (m, 2H, pip-CH_2). ^{13}C NMR (100 MHz, $CDCl_3$) δ 180.81, 167.52, 163.90, 163.11, 158.06, 136.09, 129.75, 129.28 (2C), 128.96 (2C), 113.20, 44.26 (2C), 40.70, 27.44 (2C), 23.46.

General procedure for the synthesis of thiourea derivatives (20a–b)

20 mmol of *o*-(*p*-tolyl)-chlorothionoformate **16** was added to a stirred solution of 2-aminopyrimidine **15** (20 mmol) in 30 mL acetone. The mixture was stirred continuously at RT for two hours. The completion of the reaction was verified using the TLC method. The precipitates obtained were filtered to obtain intermediate **17**, which was used for further steps without any purification. The next step involved dissolving 10 mmol of compounds **18** and **19**, 16 mmol of triethylamine, and crude intermediate **17** in 1,4-dioxane. The reaction mixture was then heated for three hours at 60 °C. After washing the resultant precipitates using diethyl ether and drying them, compounds **20a–b** were obtained.[33]

1-(2-(3-(Furan-2-ylmethyl)thioureido)-4-methyl-6-phenyl pyrimidine-5-carbonyl)piperidine-4-carboxylic acid (20a). Off-white solid, yield 70%, m.p. 195–197 °C, ^{1}H NMR (400 MHz, $CDCl_3$) δ 12.07 (s, 1H, –OH), 10.75 (s, 1H, NH), 8.73 (t, J = 3.4 Hz, 1H, NH–CH_2), 7.48 (d, J = 6.0 Hz, 2H, ArH) 7.36–7.29 (m, 5H, ArH), 7.20 (d, 1H, J = 3.6 Hz, 2H, ArH) 6.57 (dd, J = 1.6 Hz, 3.6 Hz, 2H, ArH), 4.68 (d, J = 3.4 Hz, 2H, CH_2–NH) 3.77–3.72 (m, 2H, pip-CH_2), 3.63–3.57 (m, 2H, pip-CH_2), 3.04 (*p*, 1H, J = 5.8 Hz, pip-CH), 2.56 (s, 3H, CH_3), 2.37–2.33 (m, 2H, pip-CH_2), 1.92–1.85 (m, 2H, pip-CH_2). ^{13}C NMR (100 MHz, $CDCl_3$) δ 180.8, 177.5, 167.4, 162.1, 158.9, 157.8, 154.6, 142.5, 137.0, 129.8 (2C), 129.5, 128.9 (2C), 117.3, 110.5, 107.5, 44.2 (2C), 40.7, 38.7, 27.4 (2C), 23.2. LCMS: m/z = 480.1 $[M + H]^+$; anal. calcd for $C_{24}H_{25}N_5O_4S$, C, 60.11; H, 5.25; N, 14.60; found, C, 60.20; H, 5.27; N, 14.61.

1-(4-Methyl-6-phenyl-2-(3-(thiophen-2-ylmethyl)thioureido) pyrimidine-5-carbonyl)piperidine-4-carboxylic acid (20b). Yellow solid, yield 61%, m.p. 205–207 °C, ^{1}H NMR (400 MHz, DMSO-d_6) δ 12.1 (s, 1H, –OH), 10.7 (s, 1H, NH), 8.73 (t, J = 3.3 Hz, 1H, NH–CH_2), 7.86 (d, J = 4.9 Hz, 1H, ArH), 7.35 (d, J =

4.2 Hz, 1H, ArH), 7.34–7.28 (m, 5H, ArH), 6.92 (d, $J = 4.8$ Hz, 1H, ArH), 4.68 (d, $J = 3.3$ Hz, 2H, CH_2–NH), 3.67–3.60 (m, 2H, pip-CH_2), 3.62–3.58 (m, 2H, pip-CH_2), 3.04 (*p*, 1H, $J = 5.8$ Hz, pip-CH), 2.57 (s, 3H, CH_3), 2.35–2.29 (m, 2H, pip-CH_2), 1.92–1.88 (m, 2H, pip-CH_2). ^{13}C NMR (100 MHz, DMSO-d_6) δ 181.8, 178.5, 168.4, 163.1, 159.9, 158.8, 155.6 (2C), 141.5, 138.2, 130.5, 128.9 (2C), 127.9 (2C), 119.3, 111.5, 109.5, 43.2 (2C), 41.6, 38.7, 26.4 (2C), 22.9. LC/MS: $m/z = 496.5$ $[M + H]^+$; anal. calcd for $C_{24}H_{25}N_5O_3S_2$, C, 58.16; H, 5.08; N, 14.13; found, C, 58.07; H, 5.05; N, 14.14.

Biological screening

***In vitro* antileishmanial activity.** For the *in vitro* antileishmanial assay, the promastigotes of *L. major*, *L. tropica*, and *L. donovani* were used, while for the amastigote assay, only *L. donovani* was used. The screening was done according to the reported procedure with slight modifications.[34] The amastigote forms of the parasite were produced by the reported method.[35] In brief, the parasites of each strain were cultured in tissue flasks containing the Gibco RPMI-1640 growth medium (Invitrogen) that was supplemented with 10% HIFcs (heat-inactivated fetal calf serum). The antibiotics penicillin (100 IU), streptomycin (100 μg mL^{-1}), and L-glutamine 1% (Sigma) were also added to the medium. The compounds to be tested were first uniformly dissolved in DMSO to a concentration of 1 mg mL^{-1}. Serial dilutions (three-fold) of the reference miltefosine, test sample, and standard solutions were also prepared with an appropriate concentration in fresh complete media. 100 μL culture media of 3×10^6 promastigotes of each strain, *L. major*, *L. tropica*, and *L. donovani*, were seeded in 96-well flat-bottom plates. The dilutions of compounds were introduced to their respective wells containing promastigotes. The wells containing promastigotes only were the positive control, while the wells containing 1% DMSO and the growth media alone were the negative control. After 24 h, a fluorescent dye alamarBlue (10 μL) was introduced to the respective wells and the fluorescence was measured at 630 and 540 nm after 48 h.

In the amastigote assay, serial dilutions of the synthesized compounds were made to a final concentration of 10–0.04 μg mL^{-1} using 50 μL culture media in 96-well flat-bottom plates. Then, to each well 50 μL suspension containing 2×10^3 cells per mL amastigotes was added. The plates were then incubated under 5% CO_2 at 31 °C for 72 h. After 68 hours of incubation period, 10 μL of fluorochrome solution was added to each well and absorbance was recorded at the wavelengths of 530 nm and 590 nm for excitation and emission, respectively. The experiments were carried out in triplicate. Finally, the IC_{50} values were determined from the dose–response curve using GraphPad Prism 3.0. The results were expressed as mean ± SEM of the triplicate.

Reversal of antileishmanial activity. Folate reversal was carried out as described by the previous method with slight modification.[36] In this method, trimethoprim (TOP) was utilized as a positive control. The synthesized compounds **4c** and **4g** were used in concentrations of 0.50 μM and 0.26 μM, respectively, while the folic acid was used in 100 μL and 20 μL. The assay was carried out in two stages. First, the test compounds (**4c** and **4g**) were incubated with 10^6 *Leishmania* cells suspended in a growth medium without the competitor folic acid. After 1 h, the parasite cells were washed with phosphate buffer saline (PBS), and centrifuged, media were discarded and the cells were re-suspended in a 24-well plate for incubation, counting, and calculation of percent survival. In the second stage, the same procedure was repeated with the addition of the competitor folic acid in the concentration mentioned above. Once again, the parasite cells were washed with PBS and centrifuged, media were discarded, and the cells were re-suspended in growth media for measurement of percent survival.

***In vitro* cytotoxicity testing.** This assay was carried out using normal human embryonic kidney cells (HEK-293) according to the reported method with slight modification.[37] Here, in a 96-well plate, the test compounds in the concentration range of 0.1–1 mM were added to 1×10^5 cells per well under a 5% CO_2 incubator at 36 °C for about 72 h. The culture medium (DMEM; Gibco), added with 5% heat-inactivated fetal bovine serum (HIFBS), was used as a growth medium for HEK-293 cells. Using the crystal violet method of staining, the cytotoxicity potential was determined in the form of CC_{50} value, which is the concentration of the test compound at 50% inhibition. For each compound, the experiment was performed in triplicate and GraphPad software was used for CC_{50} value calculation.

***L. major* DHFR (*Lm*DHFR) enzyme inhibition assay.** By using our previously reported method, enzyme inhibition assay was performed on cloned and over-expressed *L. major* DHFR (*Lm*DHFR).[4,38]

Docking studies

The ligand–receptor docking of the newly synthesized compounds (**4g**, **20a**, and **20b**) on *Lm*DHFR was carried out by using our previously constructed homology model,[4] while *Leishmania major* pteridine reductase 1 was retrieved with PDB ID: 2BFM. All the docking studies were performed on the Molecular Operating Environment, and the best-docked pose was visualized on Discovery Studio.

A database of the selected synthesized compounds was prepared, and energy was minimized to obtain stabilized bond angles and geometries. The database file was saved in mdb format. The site finder option of the selected active pocket of the targeted protein was done by keeping all amino acid residues as reported in the literature.[39] Furthermore, the docking procedure was validated by docking the standard drugs trimethoprim and methotrexate. The synthesized compounds were docked by retaining 20 poses for each docked ligand. The 2D interactions for the most suitable docked poses were presented, and binding energy (*S*) for each docked pose was noted.

Results and discussion

Design rationale

Thiourea derivatives in the current study have been designed in comparison to *N*,*N*-disubstituted thiourea derivative **II** (Fig. 1). The compounds **4a–h** were designed by using aniline

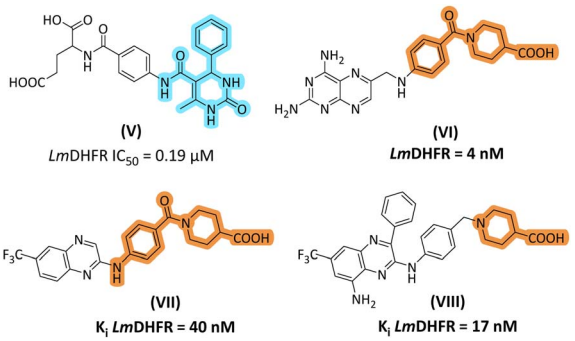

Fig. 2 Design rationale of current study based on our previously reported DHPM-2-one based inhibitor of *Lm*DHFR (**V**); piperidine-4-carboxylic acid-based inhibitors of *Lm*DHFR (**VI–VIII**).

derivatives on one side of the thiourea functionality and either a furan or thiophene ring on another side, while compounds **5a–d** were designed to accommodate 2-pyridine and 2-thiazole as R^2 substituents. Inspired by our previous study, the dihydropyrimidine-based framework has been employed to design and synthesize a series of derivatives. Biginelli type of dihydropyrimidine-2-ones (**V**) emerged as potent inhibitors of *L. major* DHFR. In the current research, we selected 2-aminopyrimidine synthesized from DHPM-2-one. The important aspect was that we modified the C-5 ester to piperidine-4-carboxylic acid to obtain **20a–b**. Piperidine-4-carboxylic acid has been reported as an important scaffold in most antileishmanial derivatives (Fig. 2).

Chemistry

All the furan/thiophene carboxylic acid derivatives (**4a–h** and **5a–d**) were synthesized as per the general scheme shown in Scheme 1. The starting materials for Scheme 1 were furan carboxylic acid, thiophene carboxylic acid, and thionyl-chloride, which were refluxed for 2–3 h, leading to the formation of the respective intermediate acid chlorides. The synthesized acid chloride intermediates were further reacted with KSCN at room temperature for 2–3 h to give isothiocyanates. The final products thiourea derivatives (**4a–4h** and **5a–5d**) were obtained by refluxing the respective isothiocyanates with substituted anilines and primary amines.

In the next step, we synthesized pyrimidine derivatives **20a–b**. For this purpose, Biginelli dihydropyrimidine derivative (**12**) was synthesized by using benzaldehyde (**10**), urea (**11**), and 1-(3-oxobutanoyl)piperidine-4-carboxylic acid (**8**, synthesized *via* Scheme 2). Pyridinium chlorochromate (PCC) was used to oxidize **12** to derivative **13**, which was further reacted with $POCl_3$ to yield 2-chloro derivative **14**.[36] 2-Chloro derivative **14** was finally reacted with ammonium acetate to give the target 2-aminopyridine derivative **15** (Scheme 3).

Finally, 2-aminopyridine-based thiourea derivatives (**20a–b**) were synthesized by the reaction of (**15**) with *o*-(*p*-tolyl)chlorothionoformate (**16**) in the first step and then with furan-2-ylmethanamine (**18**) and thiophen-2-ylmethanamine (**19**) using dioxane solvent to obtain the target thiourea derivatives **20a–b** (Scheme 4).

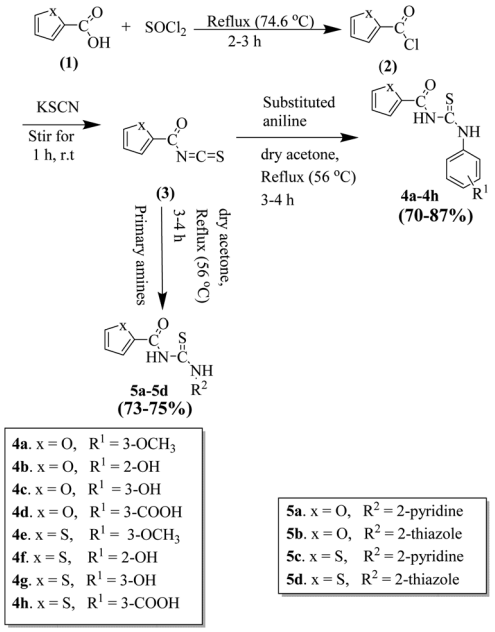

Scheme 1 Schematic for the synthesis of thiourea derivatives (**4a–4h** and **5a–5d**).

Antileishmanial assay

***In vitro* antileishmanial activity against promastigotes and amastigotes.** A total of **14** compounds were used in the assay. The *Leishmania* parasite chosen for the study includes *L. major*, *L. tropica*, and *L. donovani*. The promastigote assay was performed against all these three forms of the parasite, while the amastigote assay was performed against *L. major* only. The minimum concentration of the drug needed to inhibit 50% promastigotes or amastigotes in the exponential stage of growth is termed IC_{50}. In this assay, the activity was presented in terms of IC_{50}. Most compounds displayed considerable antileishmanial activity ranging from micromolar to submicromolar. IC_{50} values were recorded in the range of 0.14–15.06 μM against promastigote forms and 0.31–8.50 μM against amastigote forms (Table 1). The results were interesting as most of the compounds showed inhibitory potential. **4c**, **5a**, **4f**, **4g**, **5c**, **4h**, **20a**, and **20b** stand out to be the significantly active compounds in promastigote and amastigote assays. Also, these were selected to be tested for *in vivo* antileishmanial activity.

Structure–activity relationship (SAR) of thiourea derivatives concerning *in vitro* antileishmanial activity. In both

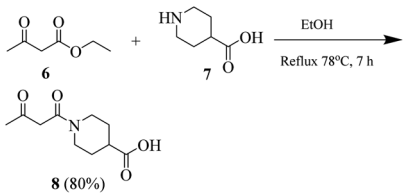

Scheme 2 Schematic for the synthesis of 1-(3-oxobutanoyl)piperidine-4-carboxylic acid (**8**).

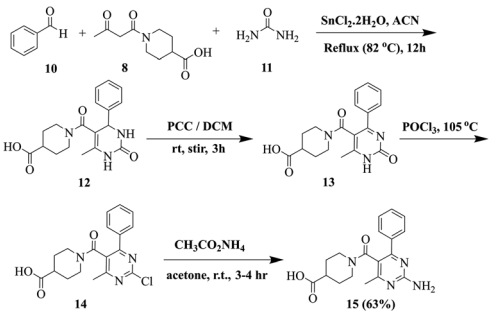

Scheme 3 Schematic for the synthesis of 2-aminopyridine derivative **15**.

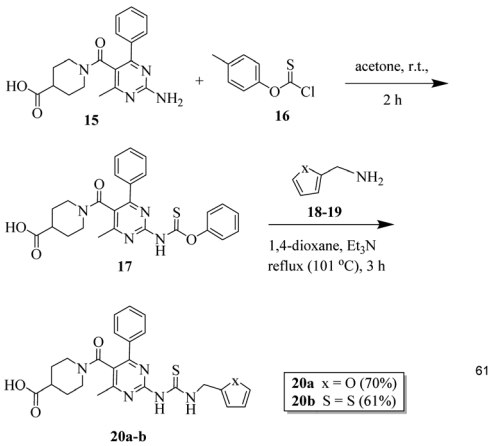

Scheme 4 Schematic for the synthesis of 2-aminopyridine-based thiourea derivatives (**20a–b**).

promastigote and amastigote assays, the activity significantly increased when the OH was positioned at the *meta*-position. The IC_{50} values of compound **4c** were 0.55 μM, 0.68 μM, and 0.48 μM for the promastigotes of *L. major*, *L. tropica*, and *L. donovani*, respectively, and 0.67 μM for the amastigotes of *L. major*. In a similar structure, the activity decreased when the phenol group's OH was positioned at the *ortho*-position, as shown for compound **4b** (IC_{50} of 6.08 μM, 4.19 μM and 2.46 μM for the promastigotes of *L. major*, *L. tropica* and *L. donovani*, respectively). It is intriguing that both activities were significantly further increased when the thiophene ring replaced the furan ring with OH positioned at the *meta*-position of the benzene ring, as shown by the compound **4f** (IC_{50} of 0.38 μM, 0.29 μM, and 0.41 μM for the promastigotes of the above mentioned three species and 0.58 μM for the amastigotes of *L. major*). Compound **4g** with OH positioned at the ortho position of the benzene also demonstrated high activity against all the tested targets (Table 1). These findings suggested that the thiophene ring linked to the phenol group through thiourea can further enhance the activity. We also anticipated that the unique groups in the thiourea compounds could serve as active pharmacophores for target recognition besides their role as physicochemical parameter modulators (molecular docking study). The compound **5c** with the pyridine ring and thiophene ring showed decreased activity against the promastigote forms of all three species. Compound **5a** also possesses a pyridine ring but the ring in this case is furan, which has also demonstrated good activity against both *L. major* promastigotes (IC_{50} = 0.97 μM) and amastigotes (IC_{50} = 8.50 μM). This reflects the role of pyridine in antileishmanial activity. The thiazole ring of compounds **5b** and **5d** displayed a decreased activity compared to the standard miltefosine.

Synthesis of a small set of 2-aminopyrimidine and furan-2-yl methanamine/thiophen-2-ylmethanamine-based thiourea analogues **20a–b** (Scheme 4) was also explored to evaluate their potential as antileishmanial agents. The synthesized analogues showed higher potency compared with the **4a–h** and **5a–d** series of compounds against *L. major* promastigotes. Analogues **20a** and **20b** also possessed good potential against the amastigotes of *L. major* with IC_{50} values of 0.47 and 0.39 μM, respectively.

In conclusion, among the **4a–h** and **5a–d** series of compounds, it has been observed that the OH group, its position, and the type of ring, whether furan or thiophene, largely affect the antileishmanial activity of these compounds. Therefore, we can conclude that the activity is determined not only by the position of the –OH group but also by the type of ring, whether thiophene or furan, which also plays a role in determining antileishmanial potential. However, **20a** and **20b** thioureas show excellent results due to the presence of an aminopyridine scaffold. Compounds **4g**, **20a**, and **20b** were selected for further studies due to their significant antileishmanial results.

***In vitro* inhibition of *L. major* dihydrofolate reductase (*Lm*DHFR) and *L. major* PTR1.** From the *in vitro* antileishmanial assays, we selected **4g**, **20a**, and **20b** to assess their inhibitory activities against *Lm*DHFR and *Lm*PTR1. 50% enzyme inhibition (IC_{50}) values were used to determine the effectiveness of the synthesized compounds. IC_{50} values of the synthesized compounds are given in Table 2.

Compounds **4g**, **20a**, and **20b** showed good inhibitory activities with IC_{50} values of 8.09, 2.63, and 1.14 μM, respectively, for *Lm*DHFR and IC_{50} values of 0.58, 15.86, and 19.89 μM, respectively, for *Lm*PTR1.

***In vivo* antileishmanial activity.** The selected compounds **4g**, **20a**, and **20b** were further explored for their *in vivo* antileishmanial activities. In this assay, $1.4 \times f10^6$ promastigotes of *L. tropica* KWH23 were used, and the results were observed after 30–120 days (Table 3). In five tested groups, there was a significant reduction in the lesion size of the mice from 0.93 ± 0.22 mm to 0.38 ± 0.18 mm after being treated with the tested sample **20a** (98.02% cure). On the other hand, the negative group displayed a mean lesion size up to 1.51 ± 0.51 mm (p > 0.05), whereas in the reference miltefosine group, the mean lesion size (end of 8th week) reduced from 0.94 ± 0.30 mm to 0.34 ± 0.40 mm. The tested samples **4g** and **20b** showed mean lesion sizes of 0.52 ± 0.80 mm to 0.32 ± 0.70 mm and 0.80 ± 0.12 mm to 0.60 ± 0.50 mm, respectively, with a corresponding percent cure rate of 91.51% and 86.28% after 8 weeks of treatment. It was proved from the results that the tested synthesized compounds exhibited potent *in vivo* antileishmanial activities against *L. tropica*. Compounds **20a** and **4g** showed significant

Table 1 Representation of *in vitro* antileishmanial activity and IC_{50} values of the synthesized compounds against the promastigotes of *L. major*, *L. tropica*, and *L. donovani* and the amastigotes of *L. major*[a]

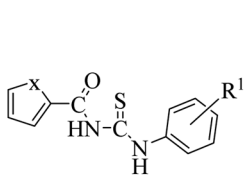

4a-4h

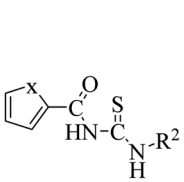

5a-5d

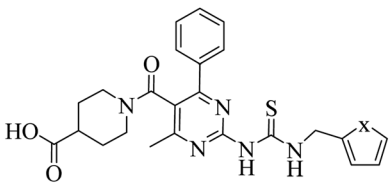

20a-b

				Antileishmanial activity IC_{50} (μM) ± SEM*			
				Promastigotes			Amastigotes
Comp. no.	R^1	R^2	X	*L. major*	*L. tropica*	*L. donovani*	*L. major*
4a	3-OCH_3	—	O	5.34 ± 0.21	7.22 ± 0.61	10.61 ± 1.12	n.d*
4b	2-OH	—	O	6.08 ± 0.14	4.19 ± 0.10	2.46 ± 0.04	n.d
4c	3-OH	—	O	0.55 ± 0.01	0.68 ± 0.05	0.48 ± 0.04	0.67 ± 0.01
4d	3-COOH	—	O	0.83 ± 0.02	1.07 ± 0.08	1.88 ± 0.11	3.24 ± 0.01
4e	3-OCH3	—	S	1.14 ± 0.05	1.23 ± 0.04	1.14 ± 0.02	n.d
4f	2-OH	—	S	0.38 ± 0.02	0.29 ± 0.01	0.41 ± 0.02	0.58 ± 0.01
4g	3-OH	—	S	0.29 ± 0.01	0.48 ± 0.02	0.24 ± 0.01	0.31 ± 0.01
4h	3-COOH	—	S	0.24 ± 0.03	0.33 ± 0.04	0.82 ± 0.04	3.04 ± 0.01
5a	—	2-Pyridine	O	0.97 ± 0.10	0.94 ± 0.06	2.30 ± 0.01	8.50 ± 0.01
5b	—	2-Thiazole	O	12.91 ± 0.42	12.38 ± 0.28	15.06 ± 0.01	n.d
5c	—	2-Pyridine	S	0.73 ± 0.09	0.79 ± 0.08	1.26 ± 0.01	n.d
5d	—	2-Thiazole	S	1.57 ± 0.04	1.53 ± 0.03	6.42 ± 0.21	n.d
20a	—	—	O	0.18 ± 0.01	n.d	n.d	0.47 ± 0.01
20b	—	—	S	0.14 ± 0.01	n.d	n.d	0.39 ± 0.01
Miltefosine				3.80 ± 0.16	2.12 ± 0.04	1.97 ± 0.07	2.89 ± 0.06

[a] $n = 3$, SEM* = standard error of mean, n.d* = not determined.

Table 2 *In vitro* inhibition results of *L. major* dihydrofolate reductase (*Lm*DHFR)[a]

IC_{50} (μM) ± SEM*		
Compound no.	*L. major* DHFR	*L. major* PTR1
4g	8.09 ± 0.01	0.58 ± 0.05
20a	2.63 ± 0.01	15.86 ± 0.01
20b	1.14 ± 0.01	19.89 ± 0.01
MTX	0.004 ± 0.000	0.173 ± 0.008

[a] SEM* = standard error of the mean ($n = 3$).

micro-molar anti-leishmanial activity with a maximum cure rate, which suggested that proceeding with further studies on these derivatives would help to gain a better insight and a profound understanding of the biological activities along with the evaluation of the safety potential of the selected candidates.

Folic acid causes a reversal of the antileishmanial activity of the active compounds. Reports revealed the potential of thio-based compounds to inhibit the leishmania enzymes dihydrofolate reductase (DHFR) and pteridine reductase (PTR1).[40] These enzymes are responsible for *Leishmania*'s resistance to available drugs. Hence, we expect that the target thiourea compounds would possibly exhibit the antileishmanial effect through folic acid pathway inhibition. This pathway in *Leishmania* involving one carbon transfer is based on an important cofactor tetrahydrofolate and another moiety pterin. The DHFR enzyme of *Leishmania* is different from human DHFR and it is responsible for the conversion of dihydrofolate to tetrahydrofolate. The parasite cell then uses this tetrahydrofolate for its growth and multiplication. It is a well-known fact that *Leishmania* species are resistant to DHFR inhibitors and they are no longer effective against *Leishmania* because of resistance.[41,42] This resistance is induced by the presence of another enzyme called pteridine reductase PTR1, which provides an alternative salvage pathway that delivers meagre folate when the DHFR-TS is blocked. Intriguingly, this salvage enzyme PTR1 is not found in human hosts and thus serves as an important target for antileishmanial drug development.[43] The antifolate mechanism of the compounds **4g**, **20a**, and **20b** was confirmed by the previous method as described with slight modification.[29] In this method, folic acid was added to the parasite first and then it was exposed to the tested compounds in the concentration above the IC_{50} values. The assay used trimethoprim as a positive control. The exposure led to almost 99% survival of the parasite, which means that our compounds act through an antifolate mechanism. It should be noted that folic acid is a substrate, and

Table 3 *In vivo* antileishmanial activities of the potent synthesized compounds[a]

Compound no.	Dose (mg kg^{-1} for five days)	(Mean, lesion, mm ± SD*) pre-treatment	Mean (lesion, mm ± SD*) post-treatment (after 8 weeks)	Percent-cure rate	Mice cured/mice infected	Survival time (mean, months)
4g	30	0.52 ± 0.80	0.32 ± 0.70	91.51%	6/6	≥2 months
20a	30	0.93 ± 0.22	0.38 ± 0.18	98.02%	6/6	≥2 months
20b	30	0.80 ± 0.26	0.60 ± 0.54	86.28%	5/6	≥2 months
Miltefosine	15	0.94 ± 0.30	0.34 ± 0.40	95.10%	6/6	≥2 months
NC	30	0.71 ± 0.51	1.51 ± 0.51	0.000%	0/6	≥2 months

[a] $n = 3$. Data are mean lesion size (mm) ± SD and SD* = standard deviation.

it competes with inhibitors for the above-mentioned enzymes DHFR and PTR1. As shown in Table 4 the antileishmanial effect of the compounds **4g**, **20a**, and **20b** was reversed upon the addition of the substrate folic acid. From this data, the compounds **4g**, **20a** and **20b** could be linked to the folate metabolism pathway targeting most probably the folate metabolism enzymes DHFR and PTR1. This was also confirmed by *in vitro* inhibition assay results (Table 2).

***In vitro* cytotoxicity testing.** Cytotoxicity assay of the three most potent compounds was performed to ascertain the safety of the synthesized derivatives. HEK-293 cells obtained from African green monkey kidney cells were used in the assay as reported by the previous method with slight modification.[30] The cells were incubated for a period of 72 h with different dilutions of the compounds **4g**, **20a**, and **20b**. The concentration at which 50% of HEK-293 cells are killed is termed CC_{50} value, which was found to be 539–786 μM (Fig. 3).

Evaluation of *in silico* studies

Docking analysis. To get an insight into the antileishmanial mechanism at the molecular level, docking studies were performed on both *in vitro* tested enzymes (*Lm*DHFR and PTR1) to explore the binding interactions. Docking studies on *Lm*DHFR were carried out on our previously reported homology-modelled enzyme, while the crystal structure of *L. major* PTR1 was obtained by using PDB ID: 2BFM. It is a tetrameric protein, where each single chain contains 288 amino acid residues and a co-crystallized ligand trimethoprim. The synthesized compounds were docked in the active pocket of target proteins with amino acid residues and the important interactions are displayed by the compounds **4g**, **20a**, and **20b**.

Docking studies on *Lm*DHFR. In the binding site of homology-modelled *Lm*DHFR, compound **4g** established two additional hydrogen bonds with amino acid residues Val156 and Asp52. In addition, one π–π stacking interaction and one π–sulphur type of hydrophobic interaction were also observed (Fig. 4a). Compound **20a** displayed hydrophobic π–π stacked interaction with Phe56, π–sulphur with Met53, and H-bond hydrophilic interactions with Ala159 and Gly42 (Fig. 4b). Compound **20b** also displayed the best binding affinities among the docked derivatives by forming five H-bond hydrophilic binding affinities with Gly43, Gly158, Asp41, Ile39, and Ala159. It also exhibited π–sulphur hydrophobic interaction with Met53 and Phe91, and π–π–T shaped interaction with Phe56 (Fig. 4c). The standard drug trimethoprim interacts with Ala32, Ile39, and Gly42 *via* hydrogen bond interactions, while Ile45 interacts with trimethoprim, forming a π–σ bond (Fig. 4d).

Docking studies on PTR-1. Docking studies were also performed on pterin reductase (PTR1) to get a deeper insight and to explore the binding interactions. The crystal structure of *Leishmania* major pteridine reductase 1 (PDB ID: 2BFM) is

Table 4 Inhibition of the folic acid pathway expressed as percentage survival

Compounds	No competitor	Folic acid	
		20 μM	100 μM
4g	[a]41%	[a]81%	[a]96%
20a	[a]45%	[a]88%	[a]98%
20b	[a]36%	[a]77%	[a]91%
Trimethoprim	[a]6%	—	[a]99%

[a] Percentage survival is obtained by the formula = 100 − %AP, where % AP is the percent of growth inhibited by either the compound or positive control. Folate activity (through the action on DHFR and PTR1) was obtained with the compounds **20a**, **20b**, and **4g**, along with a positive control trimethoprim.

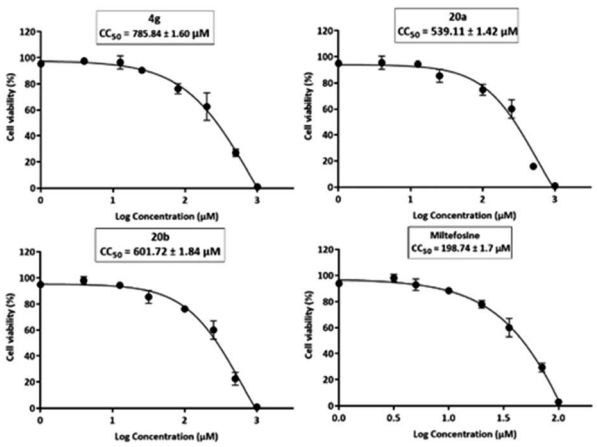

Fig. 3 Graphs of cytotoxicity concentration 50 (CC_{50}) of the final compounds (**4g**, **20a**, and **20b** and standard drug miltefosine) on HEK-293 cells.

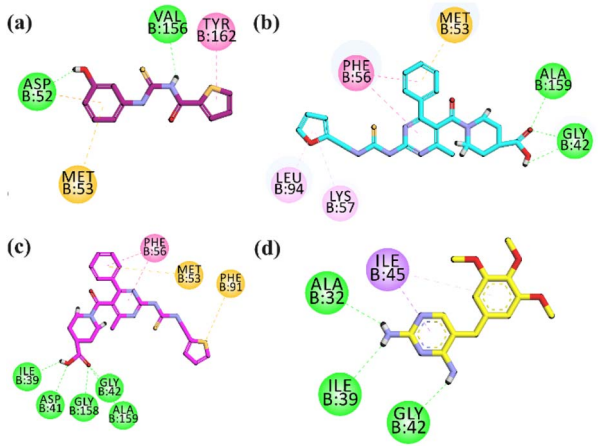

Fig. 4 Two-dimensional (2D) interaction plots of the potent compounds (a) **4g**, (b) **20a**, (c) **20b** and (d) standard drug trimethoprim in the binding region of homology modelled *L. major* DHFR.

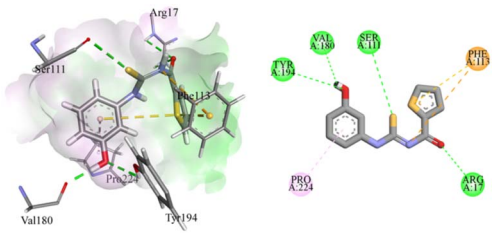

Fig. 5 Putative binding mode of compound **4g** in *Leishmania major* pteridine reductase 1 protein (PDB ID: 2BFM).

a tetrameric protein, where each single chain contains 288 amino acid residues and a co-crystallized ligand trimethoprim.

Compound **4g** was a phenol derivative that established two additional hydrogen bonds with the amino acid residues of Val180 and Tyr194. In addition, two more hydrogen bonds were found between Ser111 and thiocarbamoyl functional groups as well as between Arg17 and the oxygen of the carbamoyl group. This resulted in a significantly high binding energy of −6.8573 kcal mole^{-1}. This compound also exhibited π–sulphur and π–cation interaction with Phe113. There was also a π–alkyl interaction with Pro224, as presented in Fig. 5.

Conclusions

In this study, thiourea derivatives were designed, synthesized, and identified as antileishmanial agents in *in vitro* and *in vivo* tests. Most of the thiourea derivatives displayed moderate to high antileishmanial activity against the promastigotes of three species *L. major*, *L. tropica*, and *L. donovani*, and the amastigotes of *L. major* as compared to the reference drug miltefosine. 2-Aminopyrimidine-piperidine-4-carboxylic acid-based thiourea hybrids demonstrated excellent *in vitro* inhibition potential against the promastigotes and amastigotes of *L. major*. The selected compounds **4g**, **20a**, and **20b** also exhibited good *in vitro* results against *Lm*DHFR and *Lm*PTR1 enzymes. The reversal of antileishmanial activity by adding folic acid suggested that the compounds exert their action through the antifolate pathway, which involves the inhibition of *Leishmania* DHFR and PTR1 enzymes. The compounds appeared safe on normal human embryonic kidney cells (HEK-293). Molecular docking studies of compound **4g** on *L. major* PTR1 and compounds **4g** and **20a–b** on *L. major* DHFR presented significant interactions with specific amino acids of the surrounding pockets. The evaluation of the results showed that compounds **4g** and **20a–b** could be promising leads/hits and enrich the arsenal of antileishmanial drug development.

Ethical statement

We followed the Ethical Guidelines for Animal Testing. The Ethical Committee of the Department of Pharmacy at Bacha Khan University, Pakistan *via* departmental ethical committee number (DECN/-2023–05) approved all the protocols. All the *in vivo* experiments were conducted by the Animals Bye-Laws of 2008 (Scientific Procedure, Issue-I).

Data availability

The data supporting this article have been included as part of the ESI.†

Author contributions

YMSA and UR conceived, designed, and supervised this study. Both were involved in all the phases (from synthesis to pharmacological evaluation and manuscript writing/editing) that led to the completion of this manuscript. AH synthesized compounds with the help of MY. *In vitro* experiments were performed by AH and FH. Docking studies were performed FH and AM. Docking results were analysed and written by UR. MSJ performed *in vivo* studies. Compound characterization and cytotoxicity studies were performed at the Department of Medicinal Chemistry, University of Minnesota, Minneapolis, USA under the supervision of TS. AH, MY, and FH drafted the manuscript. YMSA and UR reviewed and edited the drafts. All the authors have read the manuscript and approved it for publication. The authors declare that there is no conflict of interest.

Conflicts of interest

The authors declare no conflict of interest.

Acknowledgements

Abdul Hadi thanks the Higher Education Commission (HEC) Pakistan for supporting the research conducted under the Faculty Development Program (FDP/FMD3-001). Abdul Hadi also thanked the Medicinal Chemistry Department at the University of Minnesota, USA for conducting a portion of his PhD research.

References

1 O. Gupta, T. Pradhan, R. Bhatia and V. Monga, *Eur. J. Med. Chem.*, 2021, **223**, 113606.
2 K. Sweiss, A. Y. Naser, M. Samannodi and H. Alwafi, *BMC Infect. Dis.*, 2022, **22**, 398.
3 M. Zucca and D. Savoia, *Open J. Med. Chem.*, 2011, **5**, 4.
4 M. Bibi, N. A. Qureshi, A. Sadiq, U. Farooq, A. Hassan, N. Shaheen, I. Asghar, D. Umer, A. Ullah and F. A. Khan, *Eur. J. Med. Chem.*, 2021, **210**, 112986.
5 A. Sabt, W. M. Eldehna, T. M. Ibrahim, A. A. Bekhit and R. Z. Batran, *Eur. J. Med. Chem.*, 2023, **246**, 114959.
6 S. Sasidharan and P. Saudagar, *Parasitol. Res.*, 2021, **120**, 1541–1554.
7 M. Akhoundi, K. Kuhls, A. Cannet, J. Votýpka, P. Marty, P. Delaunay and D. Sereno, *PLoS Neglected Trop. Dis.*, 2016, **10**, e0004349.
8 H. J. de Vries and H. D. Schallig, *Am. J. Clin. Dermatol.*, 2022, **23**, 823–840.
9 I. Abadías-Granado, A. Diago, P. Cerro, A. Palma-Ruiz and Y. Gilaberte, *Actas Dermo-Sifiliogr.*, 2021, 601–618.
10 S. Pradhan, R. Schwartz, A. Patil, S. Grabbe and M. Goldust, *Clin. Exp. Dermatol.*, 2022, **47**, 516–521.
11 D. Steverding, *Parasites Vectors*, 2017, **10**, 1–10.
12 I. Kevric, M. A. Cappel and J. H. Keeling, *Dermatol. Clin.*, 2015, **33**, 579–593.
13 G. Volpedo, R. H. Huston, E. A. Holcomb, T. Pacheco-Fernandez, S. Gannavaram, P. Bhattacharya, H. L. Nakhasi and A. R. Satoskar, *Expert Rev. Vaccines*, 2021, **20**, 1431–1446.
14 L. Monzote, *Open Antimicrob. Agents J.*, 2009, **1**, 9–19.
15 A. H. Hassan, K. Mahmoud, T.-N. Phan, M. A. Shaldam, C. H. Lee, Y. J. Kim, S. B. Cho, W. A. Bayoumi, S. M. El-Sayed and Y. Choi, *Eur. J. Med. Chem.*, 2023, **250**, 115211.
16 H. Istanbullu, G. Bayraktar, G. Karakaya, H. Akbaba, N. E. Perk, I. Cavus, C. Podlipnik, K. Yereli, A. Ozbilgin and B. D. Butuner, *Eur. J. Med. Chem.*, 2023, **247**, 115049.
17 J. A. Shiran, B. Kaboudin, N. Panahi and N. Razzaghi-Asl, *Eur. J. Med. Chem.*, 2024, 116396.
18 S. Kapil, P. Singh, A. Kashyap and O. Silakari, *SAR QSAR Environ. Res.*, 2019, **30**, 919–933.
19 D. O. Santos, C. E. Coutinho, M. F. Madeira, C. G. Bottino, R. T. Vieira, S. B. Nascimento, A. Bernardino, S. C. Bourguignon, S. Corte-Real and R. T. Pinho, *Parasitol. Res.*, 2008, **103**, 1–10.
20 N. Razzaghi-Asl, S. Sepehri, A. Ebadi, P. Karami, N. Nejatkhah and M. Johari-Ahar, *Mol. Diversity*, 2020, **24**, 525–569.
21 R. Pal, G. Teli, M. J. Akhtar and G. S. P. Matada, *Eur. J. Med. Chem.*, 2023, 115927.
22 S. B. Ansari, S. Kamboj, K. Ramalingam, R. Meena, J. Lal, R. Kant, S. K. Shukla, N. Goyal and D. N. Reddy, *Bioorg. Chem.*, 2023, **137**, 106593.
23 J. Lal, K. Ramalingam, R. Meena, S. B. Ansari, D. Saxena, S. Chopra, N. Goyal and D. N. Reddy, *Eur. J. Med. Chem.*, 2023, **246**, 114996.
24 A. Shakeel, A. A. Altaf, A. M. Qureshi and A. Badshah, *J. Drug Des. Med. Chem.*, 2016, **2**, 10.
25 P. W. Meireles, D. P. de Souza, M. G. Rezende, M. P. G. Borsodi, D. E. De Oliveira, L. C. R. P. da Silva, A. M. T. de Souza, G. M. Viana, C. R. Rodrigues and F. A. do Carmo, *Curr. Drug Delivery*, 2020, **17**, 694–702.
26 M. Sharma and P. M. Chauhan, *Future Med. Chem.*, 2012, **4**, 1335–1365.
27 B. Mohammadi-Ghalehbin, J. A. Shiran, N. Gholizadeh and N. Razzaghi-Asl, *Mol. Diversity*, 2023, **27**, 1531–1545.
28 G. M. Viana, D. C. Soares, M. V. Santana, L. H. do Amaral, P. W. Meireles, R. P. Nunes, L. C. R. P. da Silva, L. C. de Sequeira Aguiar, C. R. Rodrigues and V. P. de Sousa, *Chem. Pharm. Bull.*, 2017, **65**, 911–919.
29 M. G. Temraz, P. A. Elzahhar, A. E.-D. A. Bekhit, A. A. Bekhit, H. F. Labib and A. S. Belal, *Eur. J. Med. Chem.*, 2018, **151**, 585–600.
30 A. Mahmood, S. J. A. Shah and J. Iqbal, *Eur. J. Med. Chem.*, 2022, **231**, 114162.
31 M. A. Javed, N. Ashraf, M. Saeed Jan, M. H. Mahnashi, Y. S. Alqahtani, B. A. Alyami, A. O. Alqarni, Y. I. Asiri, M. Ikram and A. Sadiq, *ACS Chem. Neurosci.*, 2021, **12**, 4123–4143.
32 M. A. Javed, M. S. Jan, A. M. Shbeer, M. Al-Ghorbani, A. Rauf, P. Wilairatana, A. Mannan, A. Sadiq, U. Farooq and U. Rashid, *Biomed. Pharmacother.*, 2023, **159**, 114239.
33 A. Tahir, B. Mobeen, F. Hussain, A. Sadiq and U. Rashid, *RSC Adv.*, 2024, **14**, 14742–14757.
34 S. N. Khattab, N. S. Haiba, A. M. Asal, A. A. Bekhit, A. A. Guemei, A. Amer and A. El-Faham, *Bioorg. Med. Chem. Lett.*, 2017, **27**, 918–921.
35 M. Teixeira, R. de Jesus Santos, R. Sampaio, L. Pontes-de-Carvalho and W. L. dos-Santos, *Parasitol. Res.*, 2002, **88**, 963–968.
36 C. Mendoza-Martínez, N. Galindo-Sevilla, J. Correa-Basurto, V. M. Ugalde-Saldivar, R. G. Rodríguez-Delgado, J. Hernández-Pineda, C. Padierna-Mota, M. Flores-Alamo and F. Hernández-Luis, *Eur. J. Med. Chem.*, 2015, **92**, 314–331.
37 M. Tonelli, E. Gabriele, F. Piazza, N. Basilico, S. Parapini, B. Tasso, R. Loddo, F. Sparatore and A. Sparatore, *J. Enzyme Inhib. Med. Chem.*, 2018, **33**, 210–226.
38 U. Rashid, R. Sultana, N. Shaheen, S. F. Hassan, F. Yaqoob, M. J. Ahmad, F. Iftikhar, N. Sultana, S. Asghar and M. Yasinzai, *Eur. J. Med. Chem.*, 2016, **115**, 230–244.
39 F. Hussain, A. Tahir, M. S. Jan, N. Fatima, A. Sadiq and U. Rashid, *RSC Adv.*, 2024, **14**, 10304–10321.
40 E. Lebrun, Y. Tu, R. van Rapenbusch, A. R. Banijamali and W. O. Foye, *Biochim. Biophys. Acta*, 1990, **1034**, 81–85.
41 T. J. Vickers and S. M. Beverley, *Essays Biochem.*, 2011, **51**, 63–80.
42 B. Nare, L. W. Hardy and S. M. Beverley, *J. Biol. Chem.*, 1997, **272**, 13883–13891.
43 F. H. A. Leite, T. Q. Froes, S. G. da Silva, E. I. M. de Souza, D. G. Vital-Fujii, G. H. G. Trossini, S. S. da Rocha Pita and M. S. Castilho, *Eur. J. Med. Chem.*, 2017, **132**, 322–332.